

# MPPT control technology based on improved variable step conductance increment

Zhenling Li\*, Yukun Gao  
CGN New Energy Holdings Co., Ltd, Beijing, China  
\*Corresponding Author: lizhenling1976@163.com

## ABSTRACT

In order to solve the shortcomings of the traditional constant step incremental conductance method in both speed and accuracy, an improved variable step incremental conductance method is proposed. The simulation results show that compared with the traditional constant step conductance increment method, the new MPPT (maximum power point tracking) control method shows faster convergence speed and higher convergence accuracy, and effectively overcomes the limitation of the traditional method in processing optimization speed and accuracy.

**Keywords:** Maximum power point tracking, variable step size, incremental conductance method

## 1. INTRODUCTION

With the increasing contradiction between the rapid growth of social demand for energy and the aggravation of energy and environmental crisis, the proportion of renewable energy in the energy structure is increasing year by year. Photovoltaic power generation has become one of the most potential renewable energy with the characteristics of environment-friendly, clean and pollution-free, and almost unlimited resources [1]. At present, the conversion efficiency of most photovoltaic cells in the market is less than 20%. This paper studies the MPPT control of photovoltaic cells [2-3].

For the MPPT control of photovoltaics, some scholars have started relevant research. The double MPPT control method based on Bayesian inference in reference can effectively improve the tracking accuracy of maximum power point, and has good dynamic response characteristics, which is superior to the traditional disturbance observation method [4]. In reference [5], a hybrid MPPT scheme based on inversion sliding mode control with fitting optimization is proposed. The scheme first uses a cubic interpolation function, and the controller is designed based on the reference voltage and the inversion sliding mode control principle. The test results show that this method has the advantages of tracking speed and power fluctuation. In reference [6], a new optimized backstepping sliding mode controller based on integral action (BISMC) is proposed to achieve MPPT. Moreover, asymptotic stability is assured using Lyapunov stability analysis and MPPT under varying temperature and irradiance levels. The simulation results show a satisfactory performance. In reference [7], A new MPPT control strategy is proposed, which uses the linearized model parameters of photovoltaic cells as a bridge, and establishes an expression including the duty cycle on this basis. The simulation results verify the accuracy and feasibility of the proposed strategy. In reference [8], an MPPT controller based on adaptive neuro-fuzzy inference system (ANFIS) is proposed, which can obtain the optimal voltage under different temperature and radiation conditions. The technology has the advantages of high accuracy and fast optimization. Reference [9] determines the optimization range according to the constant voltage method, and the inverse cosine function method changes the optimization step to solve the problem of insufficient convergence speed and accuracy. The simulation effect is good, but the design calculation is more complex. In reference [10], A variable step conductance increment method, incorporating fuzzy algorithm, is proposed to address the tradeoff between optimization speed and accuracy. Simulation results indicate that this approach partially alleviates the conflict between optimization speed and accuracy, although its effectiveness remains limited.

## 2. PHOTOVOLTAIC CELL MODELING

### 2.1 PV module model

Photovoltaic cells are composed of multiple cells, each cell is a large area diode. The basic principle of photovoltaic power generation is photovoltaic effect. Sunlight irradiates the surface of n-type area of the diode to generate current. PV cells are typically modeled as a current source with a diode (D), a shunt resistor (RSH) for leakage, and a series resistor (rs). The equivalent circuit diagram of photovoltaic cell is shown in Figure 1.

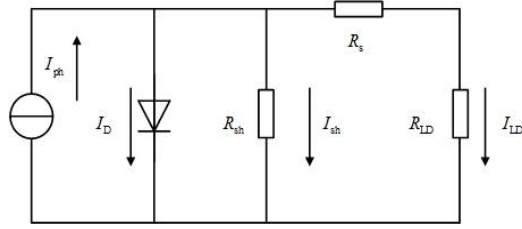


Figure 1. Equivalent circuit diagram of photovoltaic cells

According to Kirchhoff's law, the output load current can be expressed as follows:

$$I_L = I_{ph} - I_{sh} - I_D \quad (1)$$

The expression of side leakage current  $I_{sh}$  is as follows:

$$I_{sh} = \frac{U_L + I_L R_s}{R_{sh}} \quad (2)$$

The calculation formula of equivalent constant current source current  $I_{ph}$  of photovoltaic cells is as follows:

$$I_{ph} = I_{sc} \frac{S}{S_{ref}} [1 + \alpha(T - T_{ref})] \quad (3)$$

The current flowing through the diode is expressed as follows:

$$I_D = I_{D0} \left\{ \exp \left[ \frac{q(U_L + I_L R_s)}{AKT} \right] - 1 \right\} \quad (4)$$

Unknown parameters in formula (3) and formula (4):

$I_{sc}$	Short circuit current of photovoltaic cells
$S_{ref}$	Standard light intensity, 1kW / m <sup>2</sup>
$S$	Actual light intensity
$\alpha$	Temperature coefficient of current 0.144%/K
$T_{ref}$	Test temperature under standard condition, 235K
$T$	Panel temperature of photovoltaic cells
$q$	Charge quantity 1.6×10.19C
$A$	Ideal factor, generally taken as 2.8
$K$	Boltzmann constant 1.38×10.23J/K
$I_{D0}$	Diode reverse current

Formula (2), (3) and (4) are brought into formula (1) to get the following results:

$$I_L = I_{sc} \frac{S [1 + \alpha(T - T_{ref})]}{S_{ref}} - I_{D0} \left\{ \exp \left[ \frac{q(U_L + I_L R_s)}{AKT} \right] - 1 \right\} - \frac{U_L + I_L R_s}{R_{sh}} \quad (5)$$

## 2.2 Output characteristics of photovoltaic cells

The concluding phase of PV cell modeling highlights the impact of light intensity and temperature variations on the power output. In Figure 2, simulated voltage-power (U-P) and voltage-current (U-I) profiles are presented for varying light intensities, all at a standard temperature of 25°C. Notably, Figure 2a demonstrates that at lower voltage levels, the PV cell exhibits behavior similar to a stable current source. As light intensity intensifies, a clear trend emerges: the short-circuit

current rises in direct proportion. Moreover, under constant output voltage conditions, the photovoltaic cell's output current also enhances with higher light intensity. Simultaneously, Figure 2B illustrates that the maximum power point's output voltage shifts rightwards with increased light intensity, resulting in a boost to the maximum output power. Because the intrinsic light absorption coefficient of the thin film battery is as high as  $105 / \text{cm}$ , which is much higher than that of the crystalline silicon battery, the thin film battery has good low light power generation characteristics, which can make the photovoltaic battery output power effectively when the light intensity is only  $200 \text{ W} / \text{m}^2$ .

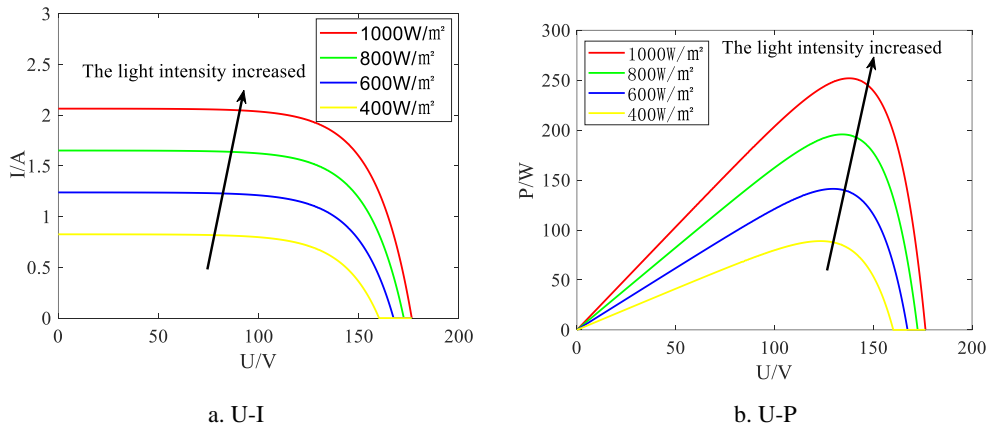


Figure 2. Output characteristic curve of photovoltaic cell under different light intensity

Figure 3 is the simulation diagram of output u-p curve and U-I curve of different PV cell body temperature under the illumination intensity of  $1 \text{ kW} / \text{m}^2$ .

As can be seen from Figure 3A, When the photovoltaic system gradually approaches the maximum power point, the decline rate of its output current will obviously change, that is, the decline trend begins to significantly slow down or turn to gentle. However, temperature has a great influence on the decreasing trend of output current when it approaches the maximum power point.

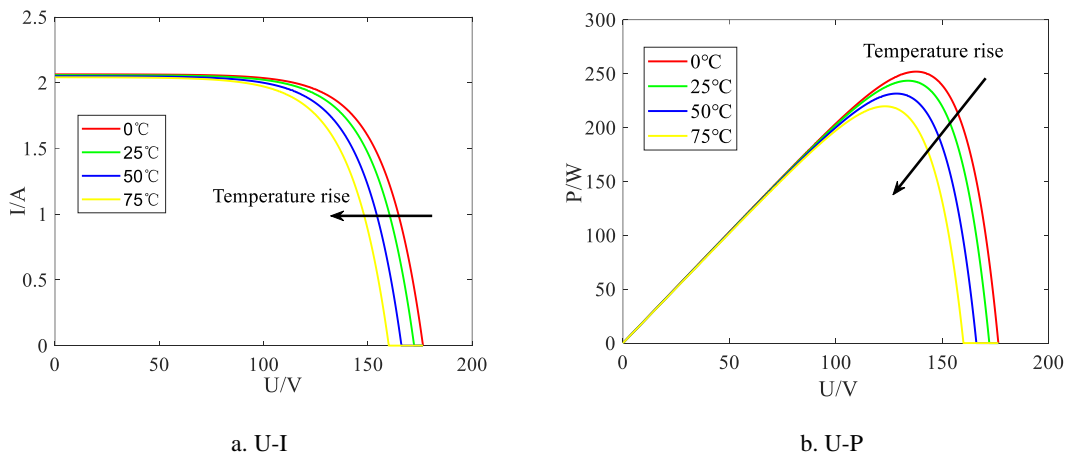


Figure 3. Output characteristic curves of photovoltaic cells at different plate temperatures

In Fig. 3b, it can be seen that with the increase of temperature, the output voltage at the maximum power point gradually moves to the left, and the maximum output power gradually decreases with the increase of temperature.

Due to the limitations of the installation, photovoltaic cells are easily affected by the shadows of surrounding buildings and plants. it is an unavoidable problem in photovoltaic, and the shadow limits the energy conversion of photovoltaic cells and could damage photovoltaic cells. In order to study the output characteristics of photovoltaic cells under shadow cover. The simulation experiments were carried out in series and parallel in two groups at  $25^\circ\text{C}$ . Each group had four photovoltaic

cells, two of which had a light intensity of  $1 \text{ kW/m}^2$ , one had a light intensity of  $400 \text{ W/m}^2$ , and the other had a light intensity of  $800 \text{ W/m}^2$ . The output  $U$ - $P$  curve is shown in Figure 4.

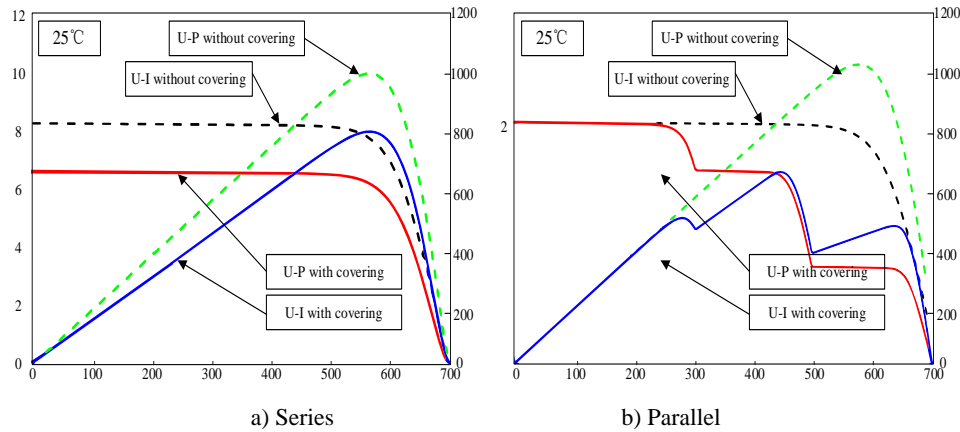


Figure 4. curves of series and parallel photovoltaic cells before and after covering

In the series connection condition, when a photovoltaic cell is shaded, the overall output power of the system is significantly dropped, the short-circuit current is significantly reduced, and the  $U$ - $P$  curve shows a multi-peak phenomenon. Under the same experimental conditions, the  $U$ - $P$  curve of the parallel photovoltaic cells is still a single peak, and the traditional MPPT control technology is still applicable. The reason is that when the light intensity decreases, the internal resistance of the photovoltaic cell increases, the output current of the branch is limited. And other photovoltaic cells on the branch cannot work at the maximum power point, the energy output of other photovoltaic cells on the branch is affected. In the parallel structure, the change of light intensity has little effect on the parallel voltage. The maximum output power of the photovoltaic cells in series after being shaded is lower than that of the parallel method.

### 3. MPPT CONTROL

After in-depth analysis, we can be clear that the output voltage of photovoltaic cells when they reach their maximum energy conversion efficiency is significantly affected by fluctuations in natural conditions such as light intensity and ambient temperature, especially changes in light intensity have a particularly significant impact on it. In view of this, ensuring the stable operation of photovoltaic cells at the maximum power point is of Paramount importance for improving their energy conversion efficiency and overall performance. In this paper, an optimized variable step size incremental conductivity algorithm is proposed to achieve this goal more accurately and efficiently.

#### 3.1 Traditional incremental conductance method

Incremental conductivity method has been widely adopted and applied in many fields because of its advantages such as simple mechanism, fast response speed and high energy efficiency conversion rate. When the derivative of the output power of the photovoltaic system to its output voltage approaches zero, it indicates that the system has reached the maximum power point [8]. The mathematical expression of the maximum power point is shown in formula (6):

$$\frac{dP}{dU} = \frac{d(UI)}{dU} = I + U \frac{dI}{dU} = 0 \tag{6}$$

Rewrite formula (6) as follows:

$$\frac{dI}{dU} = -\frac{I}{U} \tag{7}$$

When formula (7) is true, the state of the photovoltaic cell is at the maximum power point.

If the value on the left side of the formula is greater than the right side, the current point is to the left of the maximum power point. Conversely, if the value on the left side of the formula is smaller than the right side, then the current point is to the right of the maximum power point. The operation flow of the traditional incremental conductance method is shown in Figure 5, where  $C$  represents a constant perturbation step size and constant.

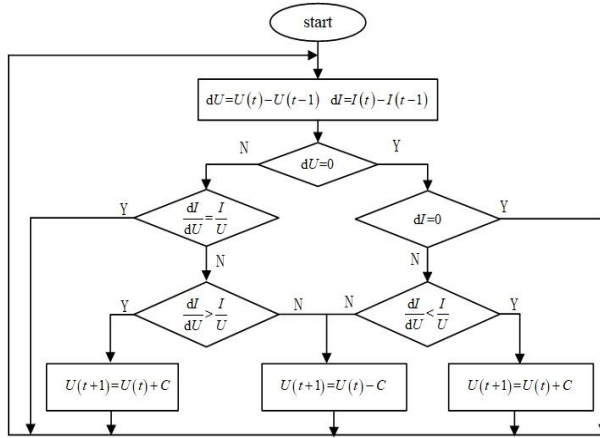


Figure 5. Flow chart of traditional incremental conductance method

### 3.2 Improved variable step incremental conductance method

The traditional MPPT control method is mostly fixed step method. The disturbance step of the fixed step method remains unchanged in the whole optimization process, which leads to the limitation of the maximum power point tracking speed. The system response speed is slow when the environment changes. At the same time, this instability will affect the accuracy of tracking, resulting in fluctuations in the output voltage of the maximum power point, and may even lead to the maximum power point being tracked in the wrong optimization direction, further reducing efficiency. A larger step size can achieve fast tracking, but it is inevitable that there will be too many steady-state oscillations. A smaller step size can reduce the oscillations with slower dynamic speed [10]. In order to solve these problems, improve the response speed of the system and the tracking accuracy of the system, many scholars have proposed the variable step size algorithm and made significant progress. In order to adapt to the dynamic characteristics of photovoltaic arrays more flexibly, the algorithm innovatively introduces a step size adaptive adjustment mechanism [11]. Based on this idea, an optimized variable step conductance increment method is proposed.

The u-p curve of photovoltaic cells is shown in Figure 6. The differential value in the figure is zero, On the right side of the maximum power point, the corresponding change curve of the absolute value of the difference shows a steeper trend, while on the left side of the maximum power point, the change of the difference is relatively flat. The differential value of phase a on the left side of the maximum power point is relatively constant, so it is unnecessary and time-consuming to optimize in a large voltage range, so it is necessary to limit the voltage optimization range to improve the optimization speed.

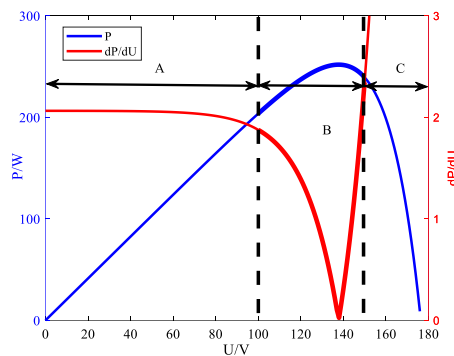


Figure 6. U-P differential curve of photovoltaic cells

Figure 6 illustrates that in transitioning to stages B and C, the differential curve notably steepens, particularly when traversing the maximum power point towards its right flank, where the absolute difference undergoes a pronounced shift, contrasting sharply with the more gradual variation observed on the left side. At this stage, too large disturbance step size is difficult to stabilize at the maximum power point, and the system stability is reduced, while too small disturbance step size slows down the system response speed. Therefore, in this stage, the variable step size algorithm is used to track the

maximum power point. In order to prevent the optimization failure caused by too large disturbance step size, the velocity factor  $n$  is introduced. The calculation formula of disturbance step size is as follows:

$$Step(t) = U(t) - U(t-1) = N \left| \frac{dP}{dU} \right| \quad (8)$$

$Step(t)$  is the disturbance step at time  $t$ ,  $U(t)$  is the output voltage at time  $t$ ,  $U(t-1)$  is the output voltage at time  $t-1$ ,  $dP = P(t) - P(t-1)$ ,  $Du = U(t) - U(t-1)$ ,  $dI = I(t) - I(t-1)$ .

When the optimization step size is excessively increased in pursuit of the fast optimization speed of the algorithm, the optimization speed of the control algorithm near the power point may be too fast, and the excessive disturbance step size leads to frequent and large amplitude over the maximum power point, resulting in severe output voltage oscillation; However, in order to stabilize the output voltage and reduce the optimization speed, the optimization speed is too slow and the system response speed is limited. Therefore, in order to improve the optimization speed and stabilize the output voltage at the same time, the power differential curve is segmented, and different optimization strategies are adopted in different regions. The schematic diagram of segmented optimization step division is shown in Figure 7.

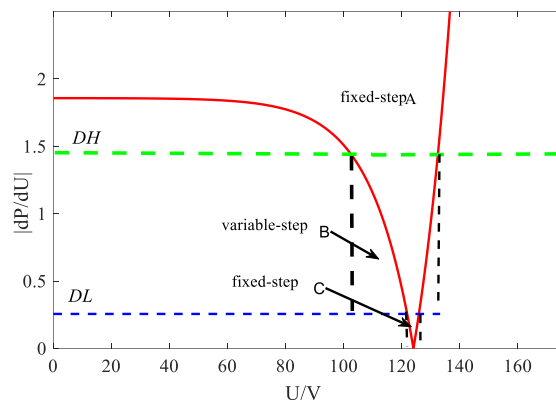


Figure 7. Schematic diagram of step size division for segmented optimization

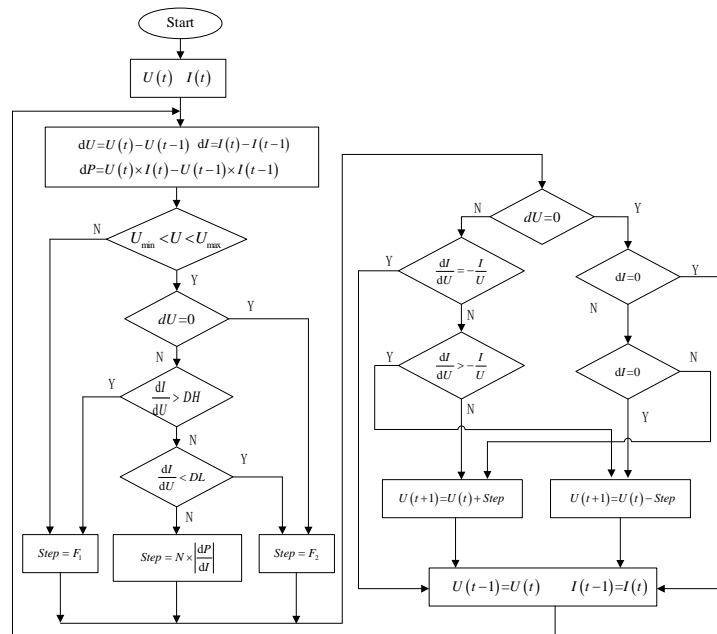


Figure 8. Flow chart of improved variable step incremental conductance algorithm

In Figure 7, the high differential value segment above the green dotted line is divided into region a, and the fixed step method with larger optimization step is adopted to improve the optimization speed; The low differential segment between

the green dashed line and the blue dashed line is divided into region B, and the output voltage is stabilized by continuous variable step size; The smaller differential value segment under the blue dotted line is divided into region C. because the differential value in this region is too small, the optimization step becomes smaller and the optimization speed is reduced. Tuning the optimization speed factor N accelerates optimization in a zone, yet excessive N risks excessive speed in B zone. To mitigate, a smaller fixed step size is adopted when the difference dips below a threshold, balancing system speed with precision demands. This refinement maintains necessary optimization velocity while enhancing accuracy. Figure 8 depicts the enhanced variable-step incremental conductance control algorithm's flowchart.

#### 4. SIMULATION ANALYSIS

##### 4.1 Parameter settings

The simulation model is shown in Figure 9, it mainly includes a photovoltaic array consisting of two photovoltaic cells in parallel, a Boost converter and a load.

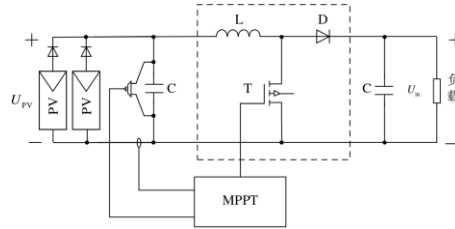


Figure 9. Simulation structure of photovoltaic system

The input voltage of the Boost converter is 80~140V, the output voltage is 380V, the maximum output power is 500W, and the operating frequency is 20kHz.

The maximum voltage gain of the Boost converter is 4.75, so the PWM duty cycle output by the drive circuit is:

$$D_{\max} = \frac{U_{\text{in}} - U_{\text{pv}}}{U_{\text{in}}} = \frac{380\text{V} - 80\text{V}}{380\text{V}} = 0.789 \quad (9)$$

In (1),  $U_{\text{PVmin}}$  is the minimum input voltage of the Boost converter, and the ripple of the output current of the converter is lower than 40%, the required inductance is:

$$L < \frac{D_{\max} U_{\text{PVmin}}^2}{0.4 f_{\text{sw}} P} = \frac{0.789 \times 80^2}{20000 \times 0.4 \times 500} = 1.26\text{mH} \quad (10)$$

Usually, the output ripple of the Boost converter should be lower than 10% of the output current. The calculation of the output filter capacitor is:

$$C > \frac{ID_{\max}}{0.1 U_{\text{in}} f_{\text{sw}}} = \frac{0.789 \times 1.37}{0.1 \times 380 \times 50000} = 5.4\mu\text{F} \quad (11)$$

In order to compare the control performance of the traditional MPPT control algorithm with the improved variable step conductance incremental method proposed in this paper, two photovoltaic cells are connected in parallel when the temperature of the photovoltaic cell body is constant, in which the light intensity of a photovoltaic cell is always  $1\text{kW} / \text{m}^2$ , and the photovoltaic cell B is covered by simulated shadow. Firstly, the initial light intensity of photovoltaic cell B is  $1\text{kW} / \text{m}^2$ . After 200ms operation, the light intensity is adjusted to  $400\text{W} / \text{m}^2$ . When the system runs to 400ms, the light intensity jumps back to  $1\text{kW} / \text{m}^2$ .

##### 4.2. Perturb and observe algorithms

As shown in Figure 10, it takes about 75ms for the output power controlled by the P&D method to reach the maximum power point. The startup speed is slow, and the output power and output voltage fluctuate greatly when the light intensity changes suddenly, the optimization accuracy is low.

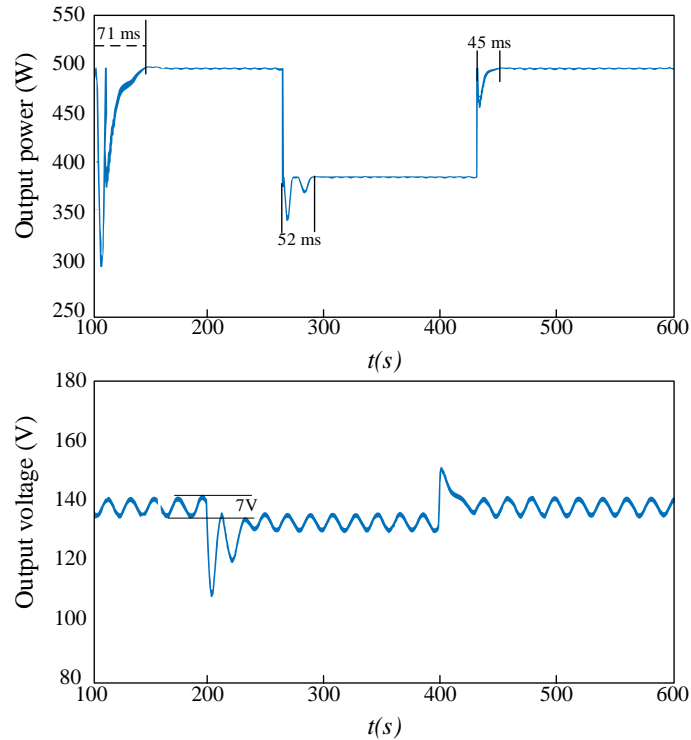


Figure 10. Output power and voltage of photovoltaic cell controlled by disturbance observation method

### 4.3 Incremental conductance

In order to comprehensively evaluate the effectiveness of the traditional incremental conductance method under different optimization strategies, we focus on the comparative analysis of its optimization speed and accuracy. the optimization step  $C$  is set as 0.2 and 0.4 respectively, and the simulation results are shown in Figure 8.

In Figure 11.a), when the optimization step  $C$  is 0.2, it takes about 18ms for the voltage to stabilize from 137V to 132V at 200ms, and 15ms for the voltage to stabilize from 132V to 137V at 400ms. The voltage fluctuation at the maximum power point is small and the optimization accuracy is high.

In Figure 11.b), when the optimization step  $C$  is 0.4, it takes about 10ms for the voltage to stabilize from 137V to 132V at 200ms, and takes about 8ms for the voltage to stabilize from 132V to 137V at 400ms. The voltage fluctuation at the maximum power point is large, and the optimization accuracy is low. To sum up, the comparative analysis shows that the optimization speed and accuracy of incremental conductance method cannot be taken into account.

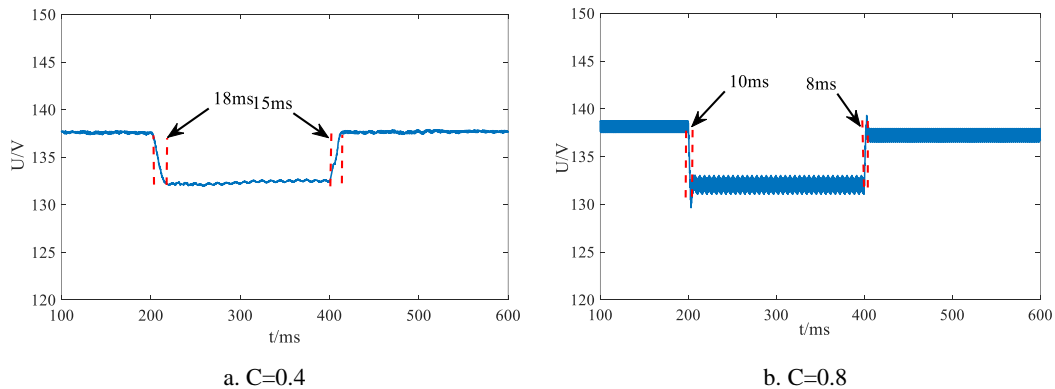


Figure 11. power variation of traditional variable step size algorithm with time



#### 4.4 Improved variable step incremental conductance method

The differential region division value  $DH = 1.25$ ,  $DL = 0.31$ , fixed step size  $F1 = 0.4$ ,  $F2 = 0.1$ , optimization speed factor  $n$  is set to 0.32. The simulation results are shown in Figure 12. It can be seen that the power fluctuation of the traditional incremental conductance method is larger after startup. The improved variable step size method shows lower output power fluctuation under steady state, while maintaining high tracking accuracy.

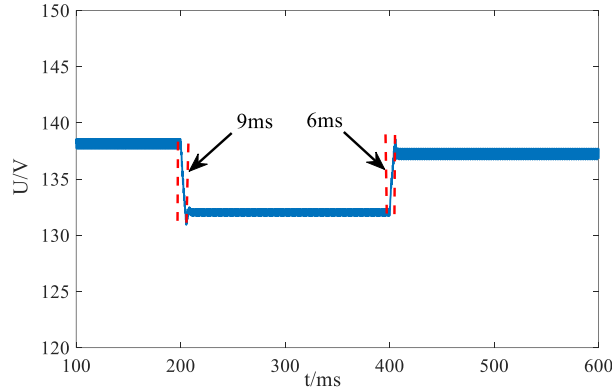


Figure 12. power variation with time of improved variable step size algorithm

When the light intensity changes from strong to weak and then back up, the improved variable step algorithm shows higher power tracking accuracy and faster response speed, and has significant performance advantages compared with the traditional variable step method. Specifically, the proposed algorithm performs better in the stability of power output, and the fluctuation range is reduced by nearly 10% compared with the traditional algorithm, thus achieving a more stable and efficient energy conversion process.

The improved variable step incremental conductance algorithm can take into account both the optimization speed and the optimization accuracy.

#### 4.5 Control test of the method

Two photovoltaic cells are connected in parallel, and one of the photovoltaic cells with smaller output power is disconnected from the grid to simulate the change in light intensity. Figure 13 shows the output voltage and current of the traditional conductance increment method and the improved method proposed in this paper respectively.

It can be seen from the figures that when the simulated light intensity changes, it can be clearly seen from the figures that compared with the traditional fixed-step conductance increment method, the improved variable step algorithm has smaller output current and voltage curve fluctuations when reaching a stable state, and the optimization speed is faster than the traditional variable step control.

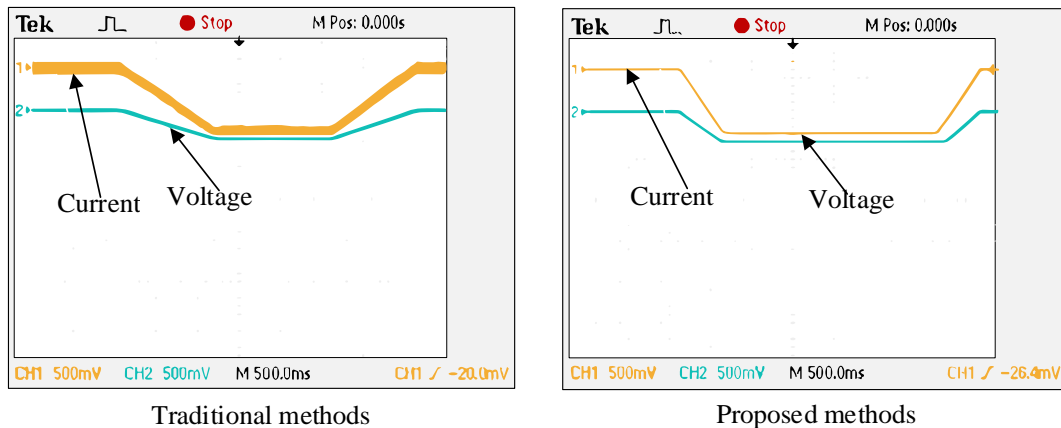


Figure 13. Output voltage and current of photovoltaic cells

## 5. CONCLUSION

Addressing the challenge of balancing optimization speed and accuracy in traditional incremental conductance methods, we introduce an enhanced approach - the refined variable step incremental conductance method. This strategy leverages an in-depth analysis of the differential characteristic curve to precisely delineate optimization zones, employing a judicious blend of fixed and variable steps. Comprehensive simulations affirm the efficacy of this innovation, which adeptly harmonizes swift optimization with precise outcomes, achieving an optimal balance between speed and accuracy.

In this paper, cadmium telluride is taken as the generation unit. It has a higher open circuit voltage and is suitable for parallel, but this does not represent all products on the market. The generalizability of the method proposed in this paper is limited, and more tests will be carried out in future research.

## REFERENCES

- [1] Li X, Xia S, Yang Y, et al. Greenness change associated with construction and operation of photovoltaic solar energy in China[J]. *Renewable energy*, 2024(May):226.
- [2] Xu Xiaorong, Yang G, Yang T, et al. Construction of 2D-2D Bi-based double heterojunctions to enhance the electrocatalytic activity of hydrogen evolution and triiodide reduction reactions[C].
- [3] Rahayu S U, Lee M W. Highly Efficient CdSe Quantum Dot-Sensitized Solar Cells via a Facile SILAR Method: Dependence of the SILAR Cycles on Optical Properties and Photovoltaic Performance[J]. IOP Publishing Ltd, 2024.
- [4] Baba A O, Liu G, Chen X. Classification and Evaluation Review of Maximum Power Point Tracking Methods[J]. *Sustainable Futures*, 2[2024-09-10].
- [5] Wang Renming, Zhang Mingrui, Bao Gang, et al. MPPT CONTROL OF PHOTOVOLTAIC SYSTEM BASED ON FITTING BACKSTEPPING SLIDING MODE METHOD[J]. *Acta Energetica Solaris Sinica*, 2023, 44(8):224-231.
- [6] Lamzouri, Ez Zahra, et al. "Optimised backstepping sliding mode controller with integral action for MPPT-based photovoltaic system using PSO technique." *International journal of computer aided engineering and technology* (2023).
- [7] Li S. An MPPT Control Strategy Based on Current Constraint Relationships for a Photovoltaic System with a Battery or Supercapacitor[J]. *Energies*, 2024, 17.
- [8] Hai T, Rezvani A, Le B N, et al. Improved design and analysis of MPPT technique for photovoltaic power systems to increase accuracy and speed under different conditions[J]. 2024.
- [9] Zhang Z, Yang B, Li Z, Li Y, Han J. "Study of MPPT Algorithm Based on New Variable Step Size Conductance Increment Method". *Power Capacitor & Reactive Power Compensation* 5(2020).
- [10] Li, X., H Wen, Hu, Y., Du, Y., & Yang, Y., "A Comparative Study on Photovoltaic MPPT Algorithms under EN50530 Dynamic Test Procedure." *IEEE Transactions on Power Electronics* PP.99(2020):1-1.
- [11] Li H., Chen C., Gao S., Li J., & Li J. "Simulation Study of Variable Step Size Incremental Conductance Based on Fuzzy Algorithm." *Automation & Instrumentation* 034.001 (2019): 84-88.